Differential top pair production at NNLO in the $q\bar{q}$ channel

Gabriel Abelof[*]

Department of Physics & Astronomy, Northwestern University, Evanston, IL 60208, USA
High Energy Physics Division, Argonne National Laboratory, Argonne, IL 60439, USA
E-mail: gabriel.abelof@northwestern.edu

Aude Gehrmann-De Ridder

Institute for Theoretical Physics, ETH, CH-8093 Zürich, Switzerland
Physics Institute University of Zürich, Winterthurerstrasse 190, CH-8057, Zürich, Switzerland
E-mail: gehra@itp.phys.ethz.ch

Imre Majer

Department of Physics and Astronomy, Seoul National University, 1 Gwanak-ro, Gwanak-gu, Seoul, 151-747, Korea
E-mail: imre.majer@alumni.ethz.ch

We report the results of our NNLO calculation for top pair hadronic production in the quark-antiquark channel, focusing on the recently derived leading-colour part. The calculation was done using an extension of the antenna subtraction method to treat massive final state fermions. We outline the integration of the relevant massive NNLO initial-final antenna functions and show differential distributions for the LHC and Tevatron.

---

[*]Speaker.

1. Introduction

With the large number of top quark pairs produced at the LHC, the study of its properties has become precision physics, and the measurement of very precise differential cross sections, attainable. Recently, the ATLAS and CMS collaborations reported measurements of differential observables in $t\bar{t}$ production in several kinematical variables, such as the transverse momentum, rapidity and invariant mass of the $t\bar{t}$ system, as well as the top quark transverse momentum and rapidity [1]. More recently, both LHC collaborations have measured the charge asymmetry in top-pair production, [2].

These measurements will allow for a very detailed and accurate probe of the top quark production mechanism. To reliably interpret data, these very precise measurements must be matched onto equally accurate theoretical predictions, which can be obtained by including contributions up to next-to-next-to leading order (NNLO) in perturbative QCD. At present, NNLO corrections have been included in calculations of the inclusive total $t\bar{t}$ cross section in [3], for the inclusive and differential Tevatron top quark forward-backward asymmetry in [4], and for differential LHC distributions in [5].

At NNLO, perturbative calculations of collider observables are typically carried out using parton-level event generators. These programs generate events for all parton-level subprocesses relevant to a given final state configuration up to NNLO accuracy and provide full kinematical information on an event-by-event basis. An NNLO event generator for observables with n final state particles or jets involves three main building blocks: the two-loop corrections to the n-parton final state, referred to as double-virtual contributions ($d\sigma_{NNLO}^{VV}$), the one-loop corrections to the $(n+1)$-parton final state, called real-virtual contributions ($d\sigma_{NNLO}^{RV}$), and the tree-level $(n+2)$-parton double real contribution ($d\sigma_{NNLO}^{RR}$). These three building blocks involve infrared divergences that arise from the exchange or emission of soft and collinear partons and cancel only in their sum. In addition, two mass factorisation counter-terms, $d\sigma_{NNLO}^{MF,1}$ and $d\sigma_{NNLO}^{MF,2}$, are needed in the three and two-parton final states contributions respectively in order to cancel infrared divergences originated from initial state collinear radiation.

The combination of subprocesses of different particle multiplicity which are individually infrared divergent is a major challenge in the construction of NNLO parton-level event generators. In our calculation this problem is dealt with using the antenna subtraction method, which was established for massless jet observables in [6], and extended to treat massive fermions in [7, 8, 9, 10]. Within the antenna subtraction framework the different contributions to a given partonic cross section are arranged as

$$d\hat{\sigma}_{NNLO} = \int_{\Phi_4} \left[d\hat{\sigma}_{NNLO}^{RR} - d\hat{\sigma}_{NNLO}^{S} \right] + \int_{\Phi_3} \left[d\hat{\sigma}_{NNLO}^{RV} - d\hat{\sigma}_{NNLO}^{T} \right] + \int_{\Phi_2} \left[d\hat{\sigma}_{NNLO}^{VV} - d\hat{\sigma}_{NNLO}^{U} \right], \quad (1.1)$$

where $d\hat{\sigma}_{NNLO}^{S}$, $d\hat{\sigma}_{NNLO}^{T}$ and $d\hat{\sigma}_{NNLO}^{U}$ are double real, one-loop virtual and double virtual subtraction terms respectively. The double real subtraction term $d\hat{\sigma}_{NNLO}^{S}$ approximates $d\hat{\sigma}_{NNLO}^{RR}$ in all its single and double unresolved limits regularising the phase space integrand, and enabling the integral to be performed in four dimensions. $d\hat{\sigma}_{NNLO}^{T}$ has the two-fold purpose of approximating $d\hat{\sigma}_{NNLO}^{RV}$ in all its single unresolved limits, while simultaneously canceling its explicit ε-poles originated from the loop integration in the real-virtual matrix elements. Finally, $d\hat{\sigma}_{NNLO}^{U}$ cancels the explicit ε-poles of the double virtual contribution $d\hat{\sigma}_{NNLO}^{VV}$.

The NNLO corrections to top pair production in the quark-antiquark channel can be decomposed into colour factors as

$$d\hat{\sigma}_{q\bar{q},\text{NNLO}} = (N_c^2 - 1)\left[N_c^2 A + N_c B + C + \frac{D}{N_c} + \frac{E}{N_c^2} + N_l\left(N_c F_l + \frac{G_l}{N_c}\right)\right.$$
$$\left. + N_h\left(N_c F_h + \frac{G_h}{N_c}\right) + N_l^2 H_l + N_l N_h H_{lh} + N_h^2 H_h\right], \qquad (1.2)$$

with N_c being the number of colours, N_l the number of light quark flavours, and N_h the number of heavy quark flavours. All coefficients multiplying the different colour factors in eq.(1.2) are gauge invariant and can be computed independently.

We computed the terms proportional to N_l in [10], in the context of a proof-of-principle calculation which showed that the antenna subtraction method can be applied to the computation of hadronic observables involving massive fermions. More recently, in [11], we concluded the evaluation of the leading-colour coefficient A which was initiated at the double real and real-virtual levels in [9], and we included the fermionic coefficients F_h, G_h, H_l, H_{lh} and H_h.

In these proceedings we shall report the results of our NNLO calculation for top pair hadronic production in the quark-antiquark channel, focusing on the leading-colour part derived in [9]. In section 2 we present the details of the integration of relevant initial-final NNLO massive antennae. In section 3 we show differential distributions for the LHC and Tevatron, and in section 4 we present our conclusions.

2. Integrated initial-final NNLO massive antennae

Antenna functions are the essential building blocks of antenna subtraction terms. They are obtained from ratios physical matrix elements, and they exist in three different types: three-parton tree-level antennae (X_3^0), four-parton tree-level antennae (X_4^0) and three-parton one-loop antennae (X_3^1). Only the latter two are genuine NNLO objects, as three-parton tree-level antennae are already needed at NLO.

By construction, antenna functions smoothly interpolate all unresolved limits of a given cluster of colour-connected partons. In the calculation of hadron collider observables, where coloured particles can be emitted off initial state legs, all three types of antennae are in principle needed in three different configurations: final-final, initial-final, and initial-initial. In addition, for processes involving massive final-state quarks massive antennae are needed, as soft radiation can be emitted of these massive particles.

In real-virtual and double virtual antenna subtraction terms, antenna functions are needed in integrated form. The integrated antennae are obtained by integrating the antenna functions over the corresponding antenna phase space inclusively. This integration is carried out analytically, and turns the implicit soft and collinear singularities of the antenna functions into explicit poles in the dimensional regularisation parameter ε, which are then cancelled against the explicit poles of the double virtual matrix elements and mass factorisation counter-terms.

For the process under consideration, namely $q\bar{q} \to t\bar{t} + X$, restricted to the colour factors that we have so far included in our calculation, the following NNLO massive antennae are needed: $A_4^0(1_Q, 3_g, 4_g, \hat{2}_q)$, $B_4^0(1_Q, 3_q, 4_{\bar{q}}, \hat{2}_{q'})$, $B_4^0(1_Q, 3_q, 4_{\bar{q}}, 2_{\bar{Q}})$ and $A_3^{1,lc}(1_Q, 3_g, \hat{2}_q)$. They are all so-called
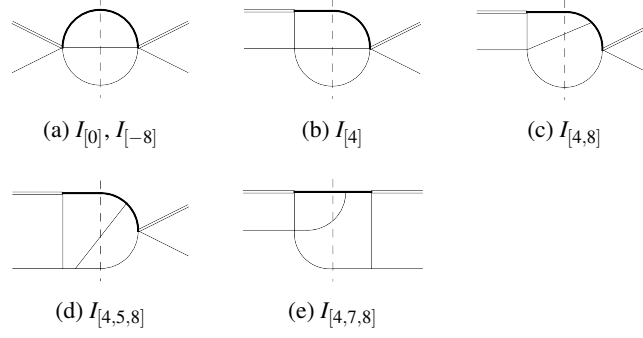
(a) $I_{[0]}$, $I_{[-8]}$ (b) $I_{[4]}$ (c) $I_{[4,8]}$

(d) $I_{[4,5,8]}$ (e) $I_{[4,7,8]}$

Figure 1: Master integrals for $\mathscr{A}^0_{q,Qgg}$. Bold (thin) lines are massive (massless). The double line in the external states represents the off-shell momentum q with $q^2 = -Q^2$. The cut propagators are the ones intersected by the dashed lines.

quark-antiquark antennae, i.e. they are derived from (crossed) matrix elements for the family of processes $\gamma^* \to q\bar{q} + $ partons. The final-final antenna $B^0_4(1_Q, 3_q, 4_{\bar{q}}, 2_{\bar{Q}})$ was derived and integrated in [12], while the initial-final antenna $B^0_4(1_Q, 3_q, 4_{\bar{q}}, \hat{2}_{q'})$ was computed and integrated in [8]. We shall here focus on the newer $A^0_4(1_Q, 3_g, 4_g, \hat{2}_q)$, and $A^{1,lc}_3(1_Q, 3_g, \hat{2}_q)$, which we derived in [9] and recently integrated in [11].

In general, integrated NNLO massive antennae are defined as

$$\mathscr{X}^1_{i,jk} = \frac{1}{C(\varepsilon)} \frac{(Q^2 + m^2_Q)}{2\pi} \int \mathrm{d}\Phi_2(p_j, p_k; p_i, q) X^l_{i,jk} \tag{2.1}$$

$$\mathscr{X}^0_{i,jkl} = \frac{1}{[C(\varepsilon)]^2} \frac{(Q^2 + m^2_Q)}{2\pi} \int \mathrm{d}\Phi_3(p_j, p_k, p_l; p_i, q) X^0_{i,jkl}, \tag{2.2}$$

with $C(\varepsilon) = (4\pi)^\varepsilon e^{-\varepsilon\gamma}/8\pi^2$. $\mathrm{d}\Phi_2$ and $\mathrm{d}\Phi_3$ are DIS-like phase spaces with kinematics of the form $p_i + q \to p_j + p_k(+p_l)$, where one of the final-state legs is massive ($p^2_k = m^2_Q$) and one of the initial-state legs is off-shell ($q^2 = -Q^2$). The inclusive integrals in eq.(2.1) are therefore functions of three scales: Q^2, $p_i \cdot q$ and m^2_Q. We parametrise the dependence on the latter two scales with the dimensionless variables

$$x_0 = \frac{Q^2}{Q^2 + m^2_Q} \qquad\qquad x = \frac{Q^2 + m^2_Q}{2p_i \cdot q}. \tag{2.3}$$

In all cases, the inclusive phase space integration is performed following the standard technique of reduction to master integrals using integration-by-parts identities (IBP) [13]. The computation of the master integrals is then carried out either directly to all-orders or iteratively, order by order in ε, using differential equations techniques [14]. All master integrals found in the reduction of $\mathscr{A}^0_{q,Qgg}$ and $\mathscr{A}^{1,lc}_{q,Qg}$ are depicted in figs. 1 and 2 respectively.

Those integrals computed with differential equations contain undetermined constants that must be fixed using externally supplied boundary conditions. When possible and consistent we fix these constants by demanding that the integral be regular in the soft limit ($x \to 1$). Otherwise, an explicit computation of the integral's soft limit provides the necessary boundary condition.

(a) $I_{[3]}$ (b) $I_{[3,5]}$ (c) $I_{[3,6]}$ (d) $I_{[4,6]}$

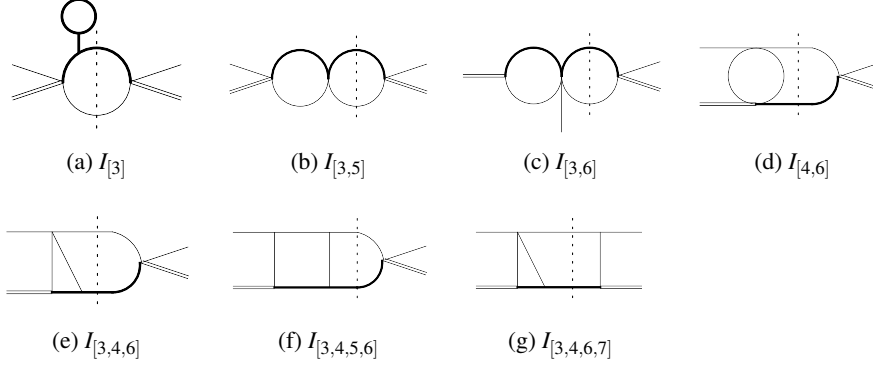(e) $I_{[3,4,6]}$ (f) $I_{[3,4,5,6]}$ (g) $I_{[3,4,6,7]}$

Figure 2: Master integrals for $\mathscr{A}_{q,Qg}^{1,lc}$. Bold (thin) lines are massive (massless). The double line in the external states represents the off-shell momentum q with $q^2 = -Q^2$. The cut propagators are the ones intersected by the dashed lines.

All master integrals found contain multiplicative factors of the form $(1-x)^{-n\varepsilon}$ which regulate soft endpoint singularities and should be kept unexpanded. All other terms can be safely expanded in ε. In some of the master integrals found in the one-loop antenna $\mathscr{A}_{q,Qg}^{1,lc}$, more than one ε-power of $(1-x)$ is encountered. Therefore, the master integrals which we denote collectively by $I_{\alpha}(x,x_0,\varepsilon)$ can be most generally expressed as:

$$I_{\alpha}(x,x_0,\varepsilon) = \sum_{n,m}(1-x)^{m-n\varepsilon}R_{\alpha}^{(n)}(x,x_0,\varepsilon). \tag{2.4}$$

The integers m and n are specific to each master integral; the functions $R_{\alpha}^{(n)}(x,x_0,\varepsilon)$ are regular as $x \to 1$ and can be calculated as Laurent series in ε.

The integrated antennae collectively denoted by $\mathscr{X}(x,x_0,\varepsilon)$ are linear combinations of master integrals with coefficients containing poles in ε as well as in $(1-x)$. After the masters have been inserted into the integrated antennae, these take the form

$$\mathscr{X}(x,x_0,\varepsilon) = (1-x)^{-1-n\varepsilon}\mathscr{R}_{\mathscr{X}}(x,x_0,\varepsilon), \tag{2.5}$$

where $\mathscr{R}_{\mathscr{X}}(x,x_0,\varepsilon)$ is a regular function as $x \to 1$ and the Laurent expansion of the singular factor $(1-x)^{-1-n\varepsilon}$ is done in the form of distributions as usual.

3. Results

We implemented the coefficients A, F_l, F_h, G_l, G_h, H_l, H_h and H_{lh} in eq.(1.2) in a Monte Carlo parton-level event generator based on the setup of eq.(1.1). Our program, written in `Fortran`, uses an adaptation of the phase space generator employed in the NNLO di-jet calculation of [15], and provides full kinematical information on an event-by-event basis, thus allowing the evaluation of differential distributions for top pair production including exact NNLO results for the quark-antiquark channel. Naturally, the calculation of total cross sections is also possible. When comparing our results for the total cross section in the quark-antiquark channel with those presented in [16] we found that the subleading colour terms absent in our computation play an important role.

We use analytic expressions for all matrix elements, subtraction terms and integrated subtraction terms involved in the calculation. As a result, at the real-virtual and virtual-virtual levels, the explicit infrared poles are cancelled analytically, and the finite remainders can be evaluated efficiently. For the real-virtual one-loop matrix elements we use `OpenLoops` [17] in combination with `CutTools` [18], whereas for the double virtual contributions we use the analytic two-loop matrix-elements of [19].

As explained in detail in [9], we renormalise the one and two-loop amplitudes of the heavy quark contributions proportional to $N_h N_c$ and N_h/N_c in eq.(1.2) using a hybrid scheme: the gluon wave functions as well as the heavy quark mass and wave functions are renormalised on-shell, while the strong coupling α_s is renormalised in the decoupling scheme ($\overline{\text{MS}}$ with N_l active flavours). To convert the two-loop amplitudes in [19], in which α_s is renormalised in the $\overline{\text{MS}}$ scheme with $N_F = N_h + N_l$ active flavours, to the decoupling scheme we perform a finite renormalisation of α_s.

In this section, we present numerical results for LHC (8 TeV) and Tevatron. All the results presented include all partonic channels at LO and NLO. At NNLO, the contributions to the quark-antiquark channel from the colour factors N_c^2, $N_l N_c$, N_l/N_c, $N_h N_c$, N_h/N_c, N_l^2, N_h^2, $N_l N_h$ and $N_h N_c$ and N_h/N_c are included. We use the pole mass of the top quark $m_t = 173.3$ GeV, and the PDF sets MSTW2008 68cl. The factorisation and renormalisation scales are set equal to the top quark mass $\mu_R = \mu_F = m_t$ throughout. Where provided, scale variations correspond to the range $m_t/2 \leq m_t \leq 2m_t$.

3.1 Differential distributions for LHC

In fig.3 we present differential distributions for top pair production in pp collisions with $\sqrt{s} = 8$ TeV at LO, NLO and NNLO, together with the corresponding k-factors. As expected, the impact of the NNLO corrections in the $q\bar{q}$ channel on LHC cross sections is in general mild, given the dominance of the gluon-gluon initiated process in this scenario.

From the ratios NNLO/NLO in the lower panels of fig. (a), it can be seen that the NNLO corrections decrease the p_T^t distributions over the entire spectra considered. The decreases range between 3% and 7%, being more pronounced in the tails of the distributions.

In the distribution in the rapidity of the $t\bar{t}$ system ($y^{t\bar{t}}$) given in figs. (b), it can be seen that in comparison with the full NLO result, NNLO corrections in the quark-antiquark channel shift the cross sections downwards in the central region by 5%. In the very forward and backwards ends of the spectrum the impact of these corrections is more substantial, causing an upwards shift over 50%. Both plots in fig.3 show a slight reduction in the scale uncertainty when the NNLO corrections to the $q\bar{q}$ channel are included.

3.2 Differential distributions for Tevatron

In fig.4 we present differential distributions for top pair production in $p\bar{p}$ collisions with $\sqrt{s} = 1.96$ TeV at LO, NLO and NNLO, along with the corresponding ratios. Given the dominance of the quark-antiquark channel in this scenario, the impact of the NNLO corrections included in our calculation is more important here than in the LHC distributions presented above. In all cases we find good agreement with experimental data, and a significant reduction in the scale uncertainty at NNLO.
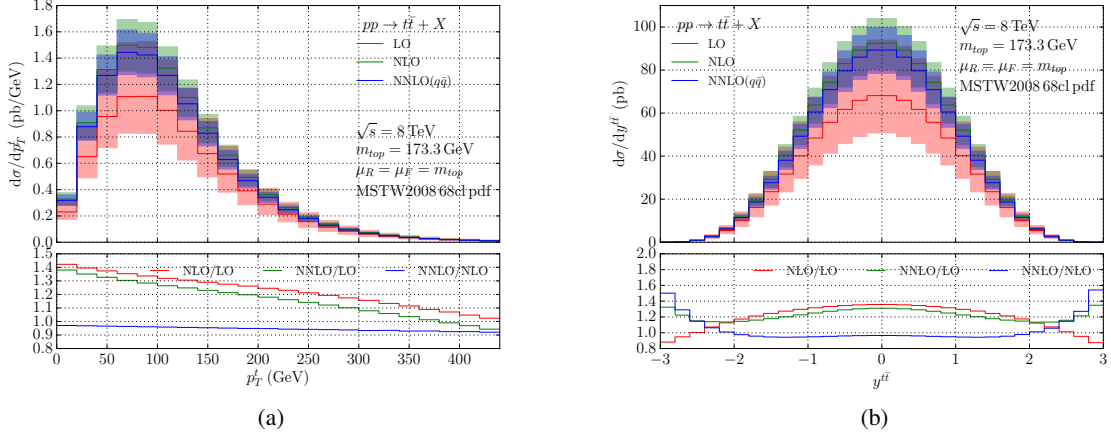
Figure 3: Differential distributions for LHC ($\sqrt{s} = 8$ TeV) in: (a) top quark transverse momentum p_T^t, (b) rapidity of the $t\bar{t}$ system $y^{t\bar{t}}$. The NNLO contributions included are in the quark-antiquark channel only. Renormalisation and factorisation scales are set equal $\mu_R = \mu_F = \mu$ and varied as $m_t/2 \leq \mu \leq 2m_t$.

As can be seen from the distribution in p_T^t given in fig.(a), in the lower part of the spectrum, NNLO corrections introduce a 10% shift with respect to the NLO prediction. This shift decreases as p_T^t increases, becoming negligible in the tail of the distribution. In fig.(b) we show the inclusive cross section for top pair hadro-production as a function of the invariant mass of the top-antitop system. NNLO corrections, in this case, cause a positive shift over the entire spectrum ranging from 15% near the production threshold to approximately 5% in the tail of the distribution.

In order to assess the relative size of the contributions from the different colour factors included at NNLO in our calculation, in fig.5 we show the breakdown of the NNLO corrections to the y^t distribution into colour factors. We find that the leading-colour piece, proportional to N_c^2, contributes most significantly, followed by $N_l N_c$, which was calculated in [9]. The contributions from all other colour factors are very small.

4. Conclusions

We presented our NNLO calculation of the differential cross section for top pair hadronic production in the quark-antiquark channel. The NNLO corrections include the leading-colour and heavy quark contributions completed recently in [11], as well as the previously computed light quark corrections [10] and other straightforward fermionic contributions.

In order to isolate and cancel the infrared divergences that arise in the various individual contributions to the NNLO cross section we employed the massive extension of the antenna subtraction method. This required the integration of new massive tree-level four-parton and three-parton one-loop antennae presented here and in [11].

The calculation was implemented as a fully differential Monte Carlo event generator, which allowed us to produce several differential distributions for top pair production with NNLO corrections in the quark-antiquark channel for Tevatron and LHC energies. In particular, we obtained
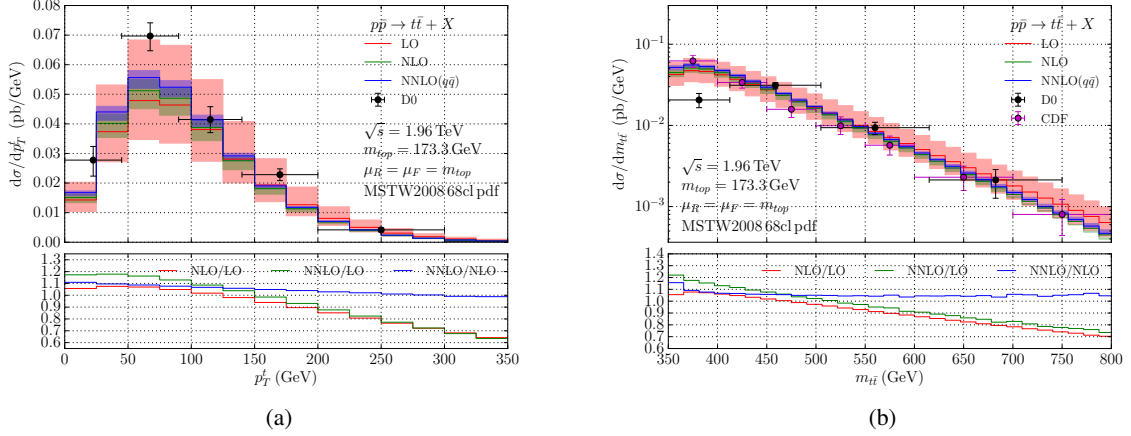
(a)   (b)

Figure 4: Differential distributions for Tevatron in: (a) top quark transverse momentum p_T^t, (b) invariant mass of the $t\bar{t}$ system $m_{t\bar{t}}$. The NNLO contributions included are in the quark-antiquark channel only. Renormalisation and factorisation scales are set equal $\mu_R = \mu_F = \mu$ and varied as $m_t/2 \leq \mu \leq 2m_t$. Experimental data points from CDF and D0 are taken from the results in the $\ell +$ jets channel presented in [20] and [21] respectively.

(a)   (b)
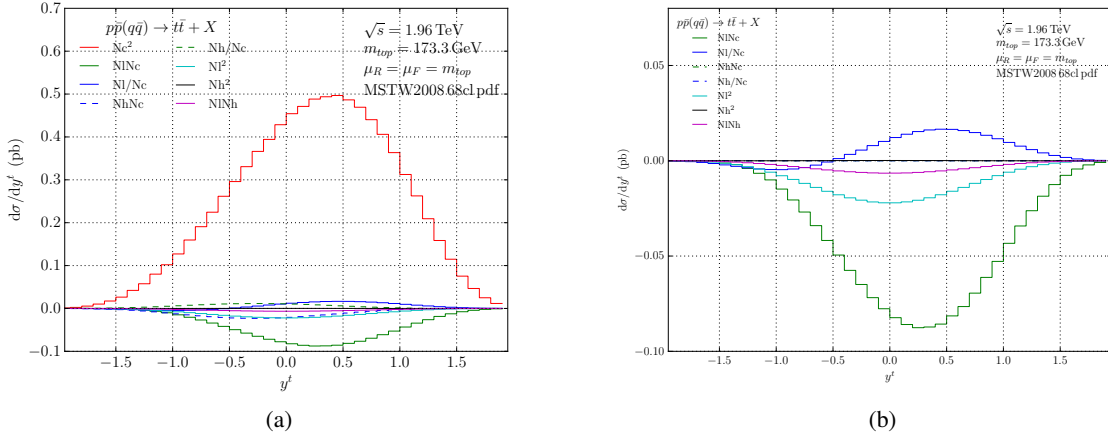
Figure 5: Contributions to the NNLO QCD corrections to $p\bar{p}(q\bar{q}) \to t\bar{t} + X$ from the different colour factors included in our computation. In (b) the leading-colour part is omitted in order to further asses the relative sizes of the various fermionic contributions.

distributions in the top quark transverse momentum p_T^t and rapidity y^t, as well as in the invariant mass and rapidity of the top-antitop system $m_{t\bar{t}}$ and $y^{t\bar{t}}$. As expected, we found that at the LHC, the NNLO corrections to the $q\bar{q}$ initiated process are not phenomenologically significant, except in the very forward and backward regions of the rapidity spectrum. For Tevatron, on the other hand, we found that these corrections are important and drastically reduce the scale dependence in all distributions considered.

Acknowledgments

References

[1] ATLAS , G. Aad *et. al.*, *Measurements of top quark pair relative differential cross-sections with ATLAS in pp collisions at* $\sqrt{s} = 7$ *TeV*, *Eur.Phys.J.* **C73** (2013), no. 1 2261 [1207.5644]; ATLAS , G. Aad *et. al.*, *Measurements of normalized differential cross sections for tt̄ production in pp collisions at* $\sqrt{s} = 7??TeV$ *using the ATLAS detector*, *Phys.Rev.* **D90** (2014), no. 7 072004 [1407.0371]; ATLAS , G. Aad *et. al.*, *Differential top-antitop cross-section measurements as a function of observables constructed from final-state particles using pp collisions at* $\sqrt{s} = 7$ *TeV in the ATLAS detector*, [1502.05923]; CMS , S. Chatrchyan *et. al.*, *Measurement of differential top-quark pair production cross sections in pp colisions at* $\sqrt{s} = 7$ *TeV*, *Eur.Phys.J.* **C73** (2013), no. 3 2339 [1211.2220]; CMS , V. Khachatryan *et. al.*, *Measurement of the differential cross section for top quark pair production in pp collisions at sqrt(s) = 8 TeV*, [1505.04480].

[2] ATLAS , G. Aad *et. al.*, *Measurement of the charge asymmetry in top-quark pair production in the lepton-plus-jets final state in pp collision data at* $\sqrt{s} = 8$ *TeV with the ATLAS detector*, [1509.02358]; CMS , V. Khachatryan *et. al.*, *Measurement of the Charge Asymmetry in Top Quark Pair Production in pp Collisions at* $\sqrt{s} = 8$ *TeV using a Template Method*, [1508.03862].

[3] M. Czakon, P. Fiedler and A. Mitov, *Total Top-Quark Pair-Production Cross Section at Hadron Colliders Through* $O(?\frac{4}{S})$, *Phys.Rev.Lett.* **110** (2013) 252004 [1303.6254].

[4] M. Czakon, P. Fiedler and A. Mitov, *Resolving the Tevatron Top Quark Forward-Backward Asymmetry Puzzle: Fully Differential Next-to-Next-to-Leading-Order Calculation*, *Phys. Rev. Lett.* **115** (2015), no. 5 052001 [1411.3007].

[5] M. Czakon, D. Heymes and A. Mitov, *High-precision differential predictions for top-quark pairs at the LHC*, [1511.00549].

[6] J. Currie, E. Glover and S. Wells, *Infrared Structure at NNLO Using Antenna Subtraction*, *JHEP* **1304** (2013) 066 [1301.4693]; A. Gehrmann-De Ridder, T. Gehrmann and N. Glover, *Antenna subtraction at NNLO*, *JHEP* **0509** (2005) 056 [hep-ph/0505111]; A. Gehrmann-De Ridder, T. Gehrmann, N. Glover and G. Heinrich, *Infrared structure of* $e^+e^- \to 3$ *jets at NNLO*, *JHEP* **0711** (2007) 058 [0710.0346]; N. Glover and J. Pires, *Antenna subtraction for gluon scattering at NNLO*, *JHEP* **1006** (2010) 096 [1003.2824]; J. Currie, A. Gehrmann-De Ridder, E. Glover and J. Pires, *NNLO QCD corrections to jet production at hadron colliders from gluon scattering*, *JHEP* **1401** (2014) 110 [1310.3993]; A. Gehrmann-De Ridder, N. Glover and J. Pires, *Real-Virtual corrections for gluon scattering at NNLO*, *JHEP* **1202** (2012) 141 [1112.3613]; A. Gehrmann-De Ridder, T. Gehrmann, E. Glover and J. Pires, *Double Virtual corrections for gluon scattering at NNLO*, *JHEP* **1302** (2013) 026 [1211.2710].

[7] G. Abelof and A. Gehrmann-De Ridder, *Antenna subtraction for the production of heavy particles at hadron colliders*, *JHEP* **1104** (2011) 063 [`1102.2443`]; G. Abelof and A. Gehrmann-De Ridder, *Double real radiation corrections to tt̄ production at the LHC: the gg → tt̄qq̄ channel*, *JHEP* **1211** (2012) 074 [`1207.6546`]; A. Gehrmann-De Ridder and M. Ritzmann, *NLO Antenna Subtraction with Massive Fermions*, *JHEP* **0907** (2009) 041 [`0904.3297`]; G. Abelof and A. Gehrmann-De Ridder, *Double real radiation corrections to tt̄ production at the LHC: the all-fermion processes*, *JHEP* **1204** (2012) 076 [`1112.4736`].

[8] G. Abelof, O. Dekkers and A. Gehrmann-De Ridder, *Antenna subtraction with massive fermions at NNLO: Double real initial-final configurations*, *JHEP* **1212** (2012) 107 [`1210.5059`].

[9] G. Abelof, A. Gehrmann-De Ridder, P. Maierhofer and S. Pozzorini, *NNLO QCD subtraction for top-antitop production in the q̄q channel*, *JHEP* **1408** (2014) 035 [`1404.6493`].

[10] G. Abelof and A. Gehrmann-De Ridder, *Light fermionic NNLO QCD corrections to top-antitop production in the quark-antiquark channel*, *JHEP* **1412** (2014) 076 [`1409.3148`].

[11] G. Abelof, A. Gehrmann-De Ridder and I. Majer, *Top quark pair production at NNLO in the quark-antiquark channel*, *JHEP* **1512** (2015) 074 [`1506.04037`].

[12] W. Bernreuther, C. Bogner and O. Dekkers, *The real radiation antenna function for S → QQ̄qq̄ at NNLO QCD*, *JHEP* **1106**, (2011) 032 [`1105.0530`]

[13] K. Chetyrkin and F. Tkachov, *Integration by Parts: The Algorithm to Calculate beta Functions in 4 Loops*, *Nucl.Phys.* **B192** (1981) 159–204; F. Tkachov, *A Theorem on Analytical Calculability of Four Loop Renormalization Group Functions*, *Phys.Lett.* **B100** (1981) 65–68.

[14] T. Gehrmann and E. Remiddi, *Differential equations for two loop four point functions*, *Nucl.Phys.* **B580** (2000) 485–518 [`hep-ph/9912329`].

[15] A. Gehrmann-De Ridder, T. Gehrmann, E. Glover and J. Pires, *Second order QCD corrections to jet production at hadron colliders: the all-gluon contribution*, *Phys.Rev.Lett.* **110** (2013), no. 16 162003 [`1301.7310`].

[16] P. Bärnreuther, M. Czakon and A. Mitov, *Percent Level Precision Physics at the Tevatron: First Genuine NNLO QCD Corrections to qq̄ → tt̄ + X*, *Phys. Rev. Lett.* **109** (2012) 132001 [`1204.5201`].

[17] F. Cascioli, P. Maierhofer and S. Pozzorini, *Scattering Amplitudes with Open Loops*, *Phys.Rev.Lett.* **108** (2012) 111601 [`1111.5206`].

[18] G. Ossola, C. G. Papadopoulos and R. Pittau, *CutTools: A Program implementing the OPP reduction method to compute one-loop amplitudes*, *JHEP* **0803** (2008) 042 [`0711.3596`].

[19] R. Bonciani, A. Ferroglia, T. Gehrmann, D. Maitre and C. Studerus, *Two-Loop Fermionic Corrections to Heavy-Quark Pair Production: The Quark-Antiquark Channel*, *JHEP* **0807** (2008) 129 [`0806.2301`]; R. Bonciani, A. Ferroglia, T. Gehrmann and C. Studerus, *Two-Loop Planar Corrections to Heavy-Quark Pair Production in the Quark-Antiquark Channel*, *JHEP* **0908** (2009) 067 [`0906.3671`].

[20] CDF , T. Aaltonen *et. al.*, *First Measurement of the t anti-t Differential Cross Section d sigma/dM(t anti-t) in p anti-p Collisions at s**(1/2)=1.96-TeV*, *Phys.Rev.Lett.* **102** (2009) 222003 [`0903.2850`].

[21] D0 , V. M. Abazov *et. al.*, *Measurement of differential tt̄ production cross sections in pp̄ collisions*, *Phys.Rev.* **D90** (2014), no. 9 092006 [`1401.5785`].